Journal of Medicinal Chemistry

Article

pubs.acs.org/jmc

Dual-Functional *abeo*-Taxane Derivatives Destabilizing Microtubule Equilibrium and Inhibiting NF-κB Activation

Yu Zhao,[†,‡,▽] Jia Su,[†,§,▽] Masuo Goto,[‡] Susan L. Morris-Natschke,[‡] Yan Li,[†] Qin-Shi Zhao,*[,†] Zhu-Jun Yao,*[,∥] and Kuo-Hsiung Lee*[,‡,⊥,#]

[†]State Key Laboratory of Phytochemistry and Plant Resources in West China, Kunming Institute of Botany, Chinese Academy of Sciences, Kunming 650204, China

[‡]Natural Products Research Laboratories, UNC Eshelman School of Pharmacy, University of North Carolina, Chapel Hill, North Carolina 27599-7568, United States

[§]Graduate School of the Chinese Academy of Sciences, Beijing 100039, China

[∥]State Key Laboratory of Bioorganic and Natural Products Chemistry, EISU Chemical Biology Division, Shanghai Institute of Organic Chemistry, Chinese Academy of Sciences, Shanghai 200032, China

[⊥]UNC Lineberger Comprehensive Cancer Center, University of North Carolina, Chapel Hill, North Carolina, 27599-7295, United States United States

[#]Chinese Medicine Research and Development Center, China Medical University and Hospital, 2 Yuh-Der Road, Taichung 40447, Taiwan

Supporting Information

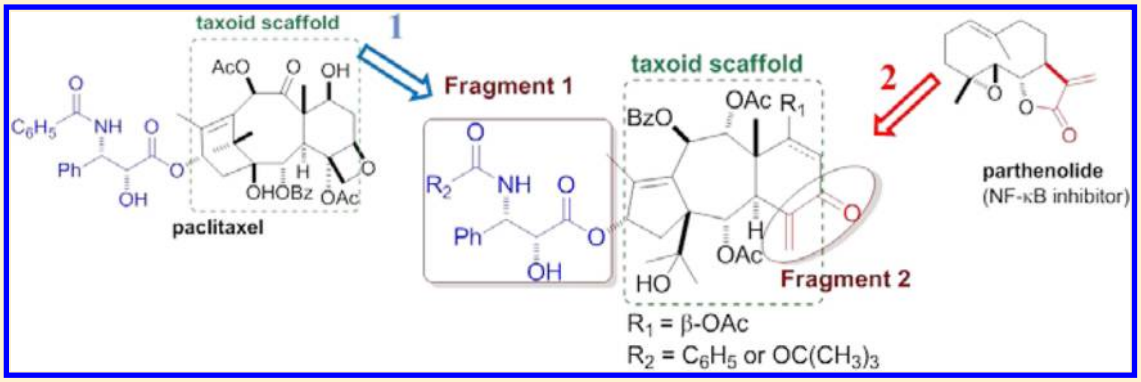

ABSTRACT: Taxchinin A, with a 11(15→1)-*abeo*-taxane skeleton, is a major, but inactive taxoid contained in leaves of *Taxus chinensis*. In our design of dual-functional antitumor *abeo*-taxane derivatives, two fragments from antitumor agents with different molecular targets (the *N*-acyl-3′-phenylisoserine side chain from the antimitotic agent paclitaxel and an α,β-unsaturated carbonyl system from NF-κB inhibitors) were incorporated into the scaffold of taxchinin A. The resulting compounds displayed broad inhibitory effects against proliferation of tumor cell lines, with notable selectivity toward colon cancer, melanoma, and renal cancer, when evaluated in the NCI-60 human tumor cell line screening panel. On the basis of the NCI-60 assay data, structure−activity relationship (SAR) correlations were elucidated. Mechanistic studies indicated that this new compound type can both destabilize microtubules and inhibit NF-κB activation, thereby inducing tumor cell apoptosis. This first report of the dual-functional taxoid-core compounds thus provides new opportunities for future drug development based on natural axoid scaffolds.

1. INTRODUCTION

Cancer is a second leading cause of death in the USA. Natural products are excellent sources of novel chemical entities and have been widely applied as leads and privileged scaffolds for elaboration into efficacious anticancer drugs.[1] Compared to single drug therapies, simultaneous effects on several targets in a related biological network often result in a superior therapeutic profile to control complex diseases including cancers.[2] However, application of multidrug combination therapy frequently leads to complex pharmacokinetic/pharmacodynamic relationships and undesired drug−drug interactions. As an alternative solution, development of appropriate single drugs to modulate multiple targets is gaining increasing interest. Among these efforts, one rational approach is to integrate corresponding structural requirements from selective ligands into a single molecule to produce new ligands that can span multiple targets.[3]

Paclitaxel (PXL) (Figure 1, Taxol, **1a**) and its semisynthetic analogue docetaxel (**1b**) have become important anticancer

Received: April 3, 2013
Published: May 31, 2013

   dx.doi.org/10.1021/jm400479p | J. Med. Chem. 2013, 56, 4749−4757

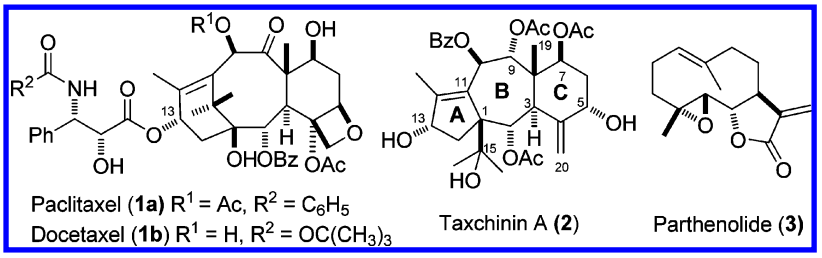

Figure 1. Structures of paclitaxel, docetaxel, taxchinin A, and parthenolide.

drugs over the past two decades. Both agents induce tubulin polymerization into microtubules and stabilize the resulting microtubules, which causes cell cycle arrest at the G2/M phase, resulting in cell apoptosis.[4] Studies on structure−activity relationship (SAR) correlations of PXL analogues have revealed that the *N*-acyl-3′-phenylisoserine side chain attached to the taxoid core at C-13 is a key pharmacophoric element.[5] To find more effective derivatives and starting materials for semisynthesis, extensive phytochemical investigations of different yew trees have identified approximately 380 taxoids with normal skeletons. Moreover, 139 taxoids with an 11(15→1)-*abeo*-taxane skeleton have been discovered primarily from *Taxus chinensis*, *T. yunnanensis*, and *T. wallichiana*.[6] However, few advances have been made in structural modification of this taxoid type, as well as corresponding studies on biological activities.[7] We isolated taxchinin A (Figure 1, **2**), a major taxoid with the *abeo*-taxane skeleton from leaves of *T. chinensis*, and accumulated it in a relatively large amount (up to 50 g). Unfortunately, taxchinin A is totally inactive against tumor cell line proliferation. In subsequent studies, we found that analogues containing taxchinin A as the core template but possessing an exocyclic unsaturated ketone in ring C exhibited satisfactory cytotoxicity.[8] To date, the mechanisms associated with the inhibitory effects of these compounds against cancer cell proliferation have not yet been disclosed.

NF-κB is a key nuclear transcription factor for tumor progression[9] and drug resistance.[10] It is often constitutively activated in human cancers. Therefore, suppression of NF-κB activation may have benefits in enhancing the efficacy of anticancer drugs and overcoming drug resistance.[11] Several NF-κB inhibitors have been employed as sensitizers in established cancer therapy over recent years. Increasing evidence has indicated that a combination of PXL with an NF-κB inhibitor, such as parthenolide (**3**, Figure 1) or curcumin, could augment the therapeutic efficacy in various cancer models.[12] Moreover, the powerful NF-κB inhibitor parthenolide and its derivatives have also been studied alone in clinical trials to treat cancer, and various studies have revealed that the α,β-unsaturated carbonyl moiety is an important structural requirement for activity.[13]

To further explore the possible therapeutic application of inactive taxchinin A and to develop potential anticancer compounds with multiple antitumor mechanisms, we proposed to integrate the *N*-acyl-3′-phenylisoserine side chain (required for microtubule binding of PXL, Figure 1) and α,β-unsaturated carbonyl unit (required for NF-κB inhibition of parthenolide, Figure 1) into the skeleton of taxchinin A. We postulated that insertion of these two drug functionalities into the *abeo*-taxane scaffold of taxchinin A might produce new unique dual-functional derivatives with potent antitumor activity (Figure 2).

According to the above proposal, four new *abeo*-taxoids were synthesized and screened against the NCI-60 cell line assay. The newly synthesized compounds exhibited a unique

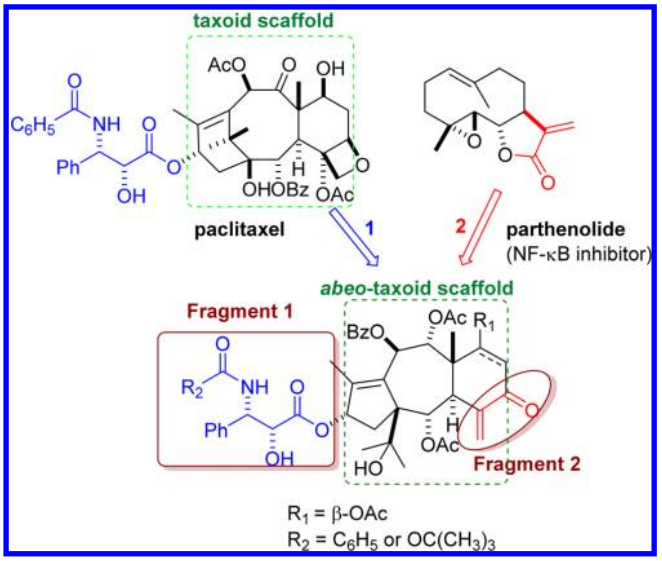

Figure 2. Design strategy for new dual-functional *abeo*-taxoid derivatives.

antitumor spectrum. Notably, further mechanistic studies supported our above hypothesis that the new taxchinin A derivatives could disrupt the microtubule equilibrium and suppress NF-κB activation simultaneously. To the best of our knowledge, this is the first report of dual functional taxoids with both microtubule destabilizing and NF-κB inhibitory activities. Also, it is a new successful example for conversion of easily available inactive taxoids into potent anticancer compounds using rational medicinal chemistry design.

2. RESULTS AND DISCUSSION

2.1. Synthesis of *abeo*-Taxoids. Syntheses of compounds **9**−**14** and **16**−**17** are shown in Scheme 1. Compound **4** was prepared from taxchinin A (**2**) in 85% overall yield in two steps using the optimized procedure we reported previously.[8] Initially, OH-13 of **2** was protected selectively by treatment with *tert*-butyldimethylchlorosilane (TBDMSCl) in imidazole and DMF. Later, the yield was increased to 90% by lowering the reaction temperature to −40 °C. Subsequent pyridinium chlorochromate (PCC) oxidation of the allylic alcohol (OH-5) provided α,β-unsaturated ketone **4**. Treatment of TBS-protected ether **4** with HF-pyridine in pyridine afforded alcohol **5** in 87% yield. Use of tetra-*n*-butylammonium fluoride (TBAF) as the deprotection reagent resulted in the production of compound **6** (90% yield), in which a new double bond was formed between C-6 and C-7 by elimination of acetic acid. Parallel acylation of the deprotected hydroxyl (OH-13) of compound **6** with β-lactams **7** and **8** afforded the products **9** and **10**, respectively. Acylation of compound **5** with **7** gave **11**, together with **9**. Compounds **12** and **10** were produced when

dx.doi.org/10.1021/jm400479p | J. Med. Chem. 2013, 56, 4749−4757

Scheme 1[a]

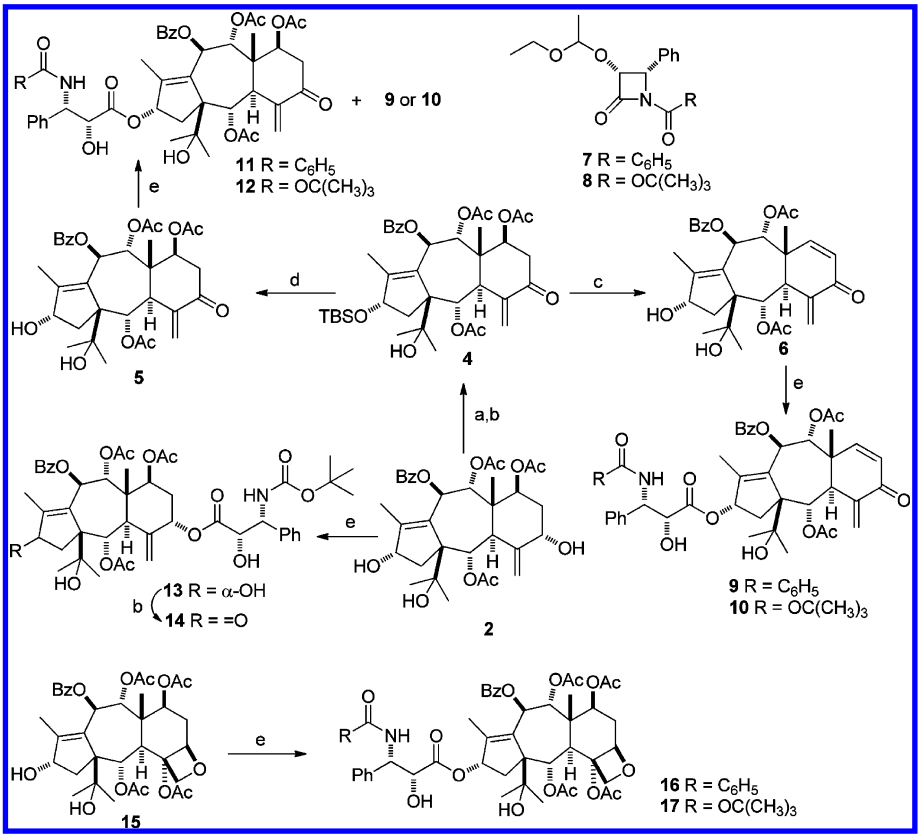

[a]Reagents and conditions: (a) TBDMSCl, DMF, −40 °C; (b) PCC, CH_2Cl_2; (c) TBAF, THF, rt; (d) HF/CH_3CN (95/5); (e) (i) NaHMDS, **7** or **8**, THF, −78 °C, (ii) 0.5 N HCl, THF, 0 °C to rt.

Table 1. GI_{50} Values from NCI-60 Human Tumor Cell Line Screening[a]

GI_{50} (μM)	9	10	11	12	13	17	1a[d]	3[d]
MOLT-4	2.48	3.78	0.65	ND[c]	83.30	42.66	0.032	15.85
NCI-H322M	4.69	24.60	18.50	18.80	NA	50.12	0.050	19.95
HCT-116	0.77	1.87	1.28	1.12	45.20	16.22	0.010	10.00
SNB-19	15.30	NA[b]	33.70	27.5	NA	33.11	0.040	63.10
LOXI MVI	1.57	2.20	1.86	1.70	NA	21.38	0.016	7.94
OVCAR-3	1.33	3.19	1.72	1.69	28.4	15.49	0.020	19.95
RXF393	0.52	2.08	1.29	1.33	26.60	12.59	0.050	12.59
DU-145	1.66	6.05	1.59	1.89	72.40	21.40	0.032	ND
T-47D	1.70	4.78	1.86	1.88	NA	38.90	0.010	ND
mean GI_{50}	2.04	8.32	2.75	2.88	70.79	27.54	0.035	17.90

[a]Data obtained from NCI-60 screening. MOLT-4, leukemia cell line; NCI-H322M, nonsmall-cell lung cancer cell line; HCT-116, colorectal carcinoma; SNB-19, CNS tumor cell lines; LOXI MVI, melanoma; OVCAR-3, ovarian cancer cell line; RXF393, renal cancer cell line; DU-145, prostate cancer cell line; T-47D, breast cancer cell line. [b]NA indicates GI_{50} value >100 μM. [c]ND indicates not determined. [d]Data can be accessed from the compound name at the following web site: http://dtp.nci.nih.gov/docs/cancer/searches/standard_agent.html.

β-lactam **8** was employed as the acylation reagent. Compound **13** was synthesized by introducing the *N*-acyl-3′-phenylisoserine side chain at the C-5 position of **2**. Subsequent oxidation of the remaining hydroxyl (OH-13) of **13** afforded compound **14**. Moreover, by using taxyunnansin A (**15**), another natural *abeo*-taxoid isolated from leaves of *T. chinensis*, rather than **2**, compounds **16** and **17**, which are *abeo*-paclitaxel and *abeo*-docetaxel derivatives, respectively, were also synthesized according to the procedures we reported previously.[14]

2.2. Antitumor Activity and SAR Study. The newly synthesized derivatives **9**−**14** and **16**−**17** were evaluated for cytotoxicity against the NCI-60 cell line panel using standard protocols.[15] Initially, these compounds were tested against the growth of 60 human tumor cell lines, including leukemia, nonsmall cell lung, colon, central nervous system (CNS), melanoma, ovarian, renal, prostate, and breast cancers, at a single dose of 10 μM. At this concentration, compounds **14** and **16** were found to be totally inactive. The six remaining compounds (**9**−**13**, **17**), which exhibited more than 50% growth inhibition at 10 μM, were further evaluated to determine their GI_{50} (50% growth inhibition) values, and the results are summarized in Table 1 and Supporting Information Figure S1.

dx.doi.org/10.1021/jm400479p | J. Med. Chem. 2013, 56, 4749−4757

Four designed compounds (**9**–**12**) exhibited broad inhibitory effects against tumor cell proliferation. Although they were largely less potent than PXL, they showed rather high potency in comparison with parthenolide (**3**) and their nontoxic parent taxchinin A (**2**). Moreover, on the basis of the mean graph obtained for all cell lines at the GI_{50} level, these compounds also exhibited unique activity patterns (Supporting Information Figure S1). In general, among the nine types of human tumor cell lines used in the screening, the colon, melanoma, and renal tumor cell lines were particularly sensitive to this compound series, while the cell lines from nonsmall-cell lung cancer and central nervous system tumor were relatively resistant. The most potent derivative **9** preferentially inhibited the proliferation of the colorectal carcinoma cell line HCT-116 and the renal tumor cell line RXF393, with GI_{50} values of 0.77 and 0.52 μM, respectively. In addition, compounds **10** and **11** were also potent against the growth of leukemia cell lines. Compound **11** strongly inhibited the proliferation of the leukemia cell line MOLT-4 (GI_{50} 0.65 μM).

Preliminary SAR conclusions were proposed on the basis of the above results (Figure 3). Compounds **9**–**12**, which contain an exocyclic unsaturated ketone moiety, showed wide ranging inhibitory effects against the tested tumor cell lines, while compounds **13**–**14** and **16**–**17**, without an exocyclic unsaturated ketone moiety, were inactive. In compounds **12** and **14**, the positions of the two important functionalities, the *N*-acyl-3′-phenylisoserine side chain and α,β-unsaturated carbonyl moiety, are interchanged. Compound **12**, with the phenylisoserine side chain at the C-13 position (A-ring) and an exocyclic unsaturated ketone moiety in the C-ring, exhibited high inhibitory potency (mean GI_{50} 2.88 μM), while compound **14**, with the phenylisoserine side chain at the C-5 position (C-ring) and an endocyclic unsaturated ketone moiety in the A-ring, was totally inactive. Compounds **11** and **12** exhibited good activity with mean GI_{50} values of 2.75 and 2.88 μM, whereas compounds **16** and **17**, with an oxetane ring on ring C, rather than the exocyclic α,β-unsaturated carbonyl system at the same position found in **11** and **12**, respectively, were inactive or weakly active. These results strongly suggested that an exocyclic α,β-unsaturated ketone moiety located in the C-ring is an essential functionality for activity. Moreover, a phenylisoserine moiety on C-13 (A-ring) is also important for activity, and minor changes of this functionality could greatly impact the activity. Among the tested compounds, analogue **9** with a C-13 *N*-benzoyl-3′-phenylisoserine side chain and a double bond between C-6 and C-7 exhibited the highest potency (mean GI_{50} 2.04 μM). The parallel compound **10**, in which a *N*-*t*-butoxycarbonyl moiety has replaced the *N*-benzoyl group of **9**, showed 4-fold lower activity. Interestingly, this potency difference was not apparent between compounds **11** and **12**, which have a saturated bond between C-6 and C-7 with an acetoxy group on C-7. Further analysis showed that, when a C-13 *N*-benzoyl-3′-phenylisoserine side chain was present (**11** vs **9**), introduction of a double bond between C-6 and C-7 did not greatly affect the activity based on mean GI_{50} values. However, in the compounds with a C-13 *N*-*t*-butoxycarbonyl-3′-phenylisoserine (**12** vs **10**), the presence of the double bond in the latter compound resulted in decreased activity.

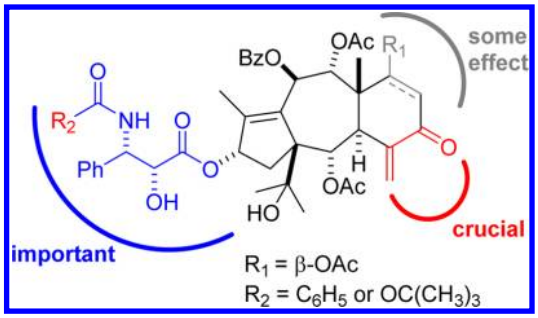

Figure 3. SAR of taxoid-based derivatives.

2.3. Apoptosis of the HCT-116 Cells Induced by Compounds 11 and 12. We then explored the mechanisms

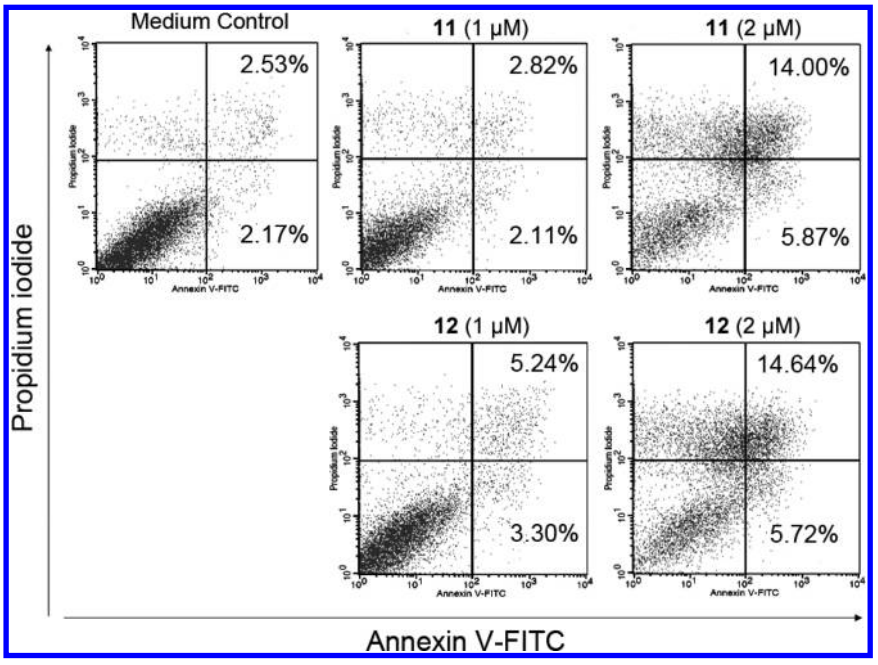

Figure 4. Compounds **11** and **12** induce apoptosis of HCT-116 cells. Cells were treated with **11** or **12** for 24 h. Treatment with **11** and **12** increased the early apoptotic (Annexin V+/PI−, lower right quadrant) and late apoptotic (Annexin V+/PI+, upper right quadrant) cells.

dx.doi.org/10.1021/jm400479p | *J. Med. Chem.* 2013, 56, 4749–4757

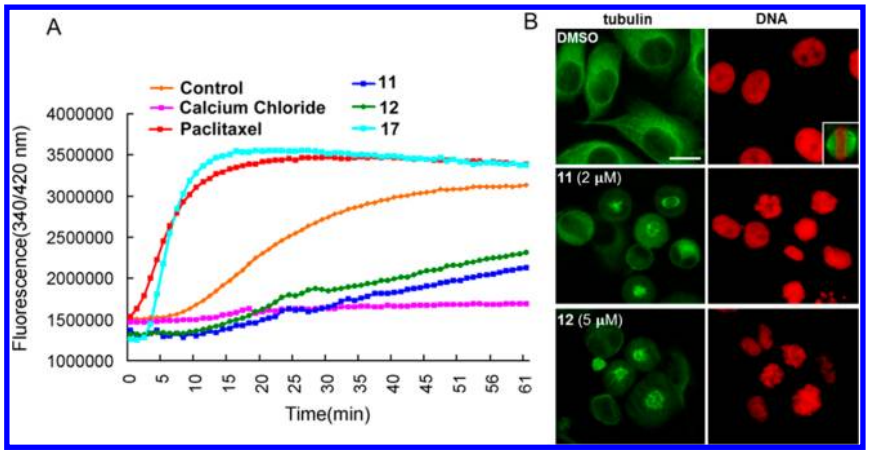

Figure 5. Effects of compounds on microtubule assembly. (A) Effects of compounds on tubulin polymerization in a cell-free system. Tubulin polymerization was detected in a fluorescence-based cell-free system in the presence of DMSO (control), 500 μM $CaCl_2$, 3 μM paclitaxel, 15 μM **11**, 15 μM **12**, or 30 μM **17**. Tubulin polymerization was measured by fluorescence intensity at 420 nm emission and 340 nm excitation. Data are representative of three independent experiments performed in triplicate. (B) Effects of compounds on microtubule dynamics in PC-3 cells. PC-3 cells were cultured and treated with DMSO (control), 2 μM compounds **11**, or 5 μM compound **12** for 24 h. Cells were stained with monoclonal antibody to α-tubulin and DAPI for DNA. The inset (upper panel) shows a typical image of metaphase cell with spindles. Cells with abnormal spindles and microtubules were detected among the cells treated with compound **11** or **12**. Although both compounds gave similar defects on tubulin dynamics, significant effects were not seen in cells treated with 2 μM **12**. Additional images are available in Supporting Information Figure S2. Bar, 25 μm.

of action of these new *abeo*-taxane derivatives. Initially, compounds **11** and **12** were examined for apoptosis-induction ability. We used the HCT-116 cell line due to its sensitivity to this compound series. Compounds **11** and **12** showed antiproliferative activity against HCT-116 cells with GI_{50} values of 1.28 and 1.12 μM, respectively (Table 1). Apoptosis in HCT-116 cells was induced by treatment with compound **11** or **12** in a dose-dependent manner. Apoptotic cell number increased to 8.54% and 20.36% when the cells were treated with compound **11** at 1 and 2 μM, and to 4.93% and 19.87% for compound **12** at 1 and 2 μM, respectively (Figure 4). These results indicated that the antiproliferative activity of **11** and **12** against HCT-116 cells might result from their ability to induce apoptosis.

2.4. Tubulin Polymerization Assay. Because the new derivatives have the unique *abeo*-taxane core as well as a phenylisoserine side chain at C-13, we also tested them for direct effects on tubulin polymerization in a cell-free system, in comparison with PXL and *abeo*-docetaxel derivative **17**. Compounds **11** and **12** interfered with microtubule assembly quite differently from PXL or **17** (Figure 5A). In accordance with previous reports,[9,12,13] PXL induced tubulin polymerization and **17** exhibited a similar effect. Surprisingly, compounds **11** and **12** displayed microtubule destabilizing potency comparable to Ca^{2+}-induced depolymerization. This finding is unusual because various known derivatives of PXL (including *abeo*-paclitaxel) have commonly been found to display microtubule stabilization activity.[5,7a,c,e] To the best of our knowledge, our finding is the first report of taxoid-core derivatives that clearly inhibit tubulin polymerization. The above results imply that these two compounds should interact directly with tubulin and/or microtubules in a different manner from that of PXL and **17**, even though the only structural difference between compounds **17** and **12** is the replacement of the oxetane ring in **17** with an exocyclic unsaturated carbonyl functionality in **12**. This minor structural alteration led to opposite effects on tubulin polymerization. In other words, these two compounds could serve as a pair of "molecular switches" (**12** for destabilization, **17** for stabilization of microtubules). In addition, we suppose that the unsaturated carbonyl unit in **12** could either react in a Michael-type addition with a thiol group on microtubules or induce a conformational change that might affect the binding mode of **12** to microtubules and, thus, produce a different effect on tubulin polymerization. Overall, such findings should be helpful in understanding how taxoids and their derivatives interact with microtubules.

When PC-3 prostate cancer cells were treated with **11** and **12**, an immunofluorescence staining assay showed morphological changes in the microtubules (Figure 5B). Combretastatin A4 (CA4) and PXL were also evaluated as positive controls (Supporting Information Figure S2). PXL induced overpolymerized microtubules in a bundled sheet-like pattern, while CA4, which binds to the colchicine-binding site, led to complete depolymerization of the microtubular network. Tubulin immunofluorescence staining of **11**- or **12**-treated mitotic cells indicated that these cells failed to assemble a typical mitotic spindle, while microtubules in interphase cells were not significantly disrupted. This phenotype was clearly different from that of CA4- or PXL-treated cells. In addition, **11**- or **12**-treated mitotic cells contained condensed chromatin, which failed to align at the metaphase plate, and were confirmed as prometaphase by staining with 4′,6-diamidino-2-phenylindole (DAPI). These observations demonstrated that **11** and **12** induce cell cycle arrest at prometaphase, which agrees with accumulation at G2/M phase as analyzed by flow cytometry.

Cell cycle arrest in the G2/M phase is a characteristic effect of many antimitotic agents that disrupt microtubule assembly.[16] To obtain further evidence that the new derivatives function by tubulin-interacting mechanisms, HCT-116 cells were treated with **11** and **12** for 12 h and evaluated by a PI staining-based fluorescence-activated cell sorting analysis. As postulated, compounds **11** and **12** caused dose-dependent accumulation of G2/M cells, accompanied with a reduction of G0/G1 cells (Figure 6). After treatment with compounds **11** and **12** at 2

dx.doi.org/10.1021/jm400479p | J. Med. Chem. 2013, 56, 4749−4757

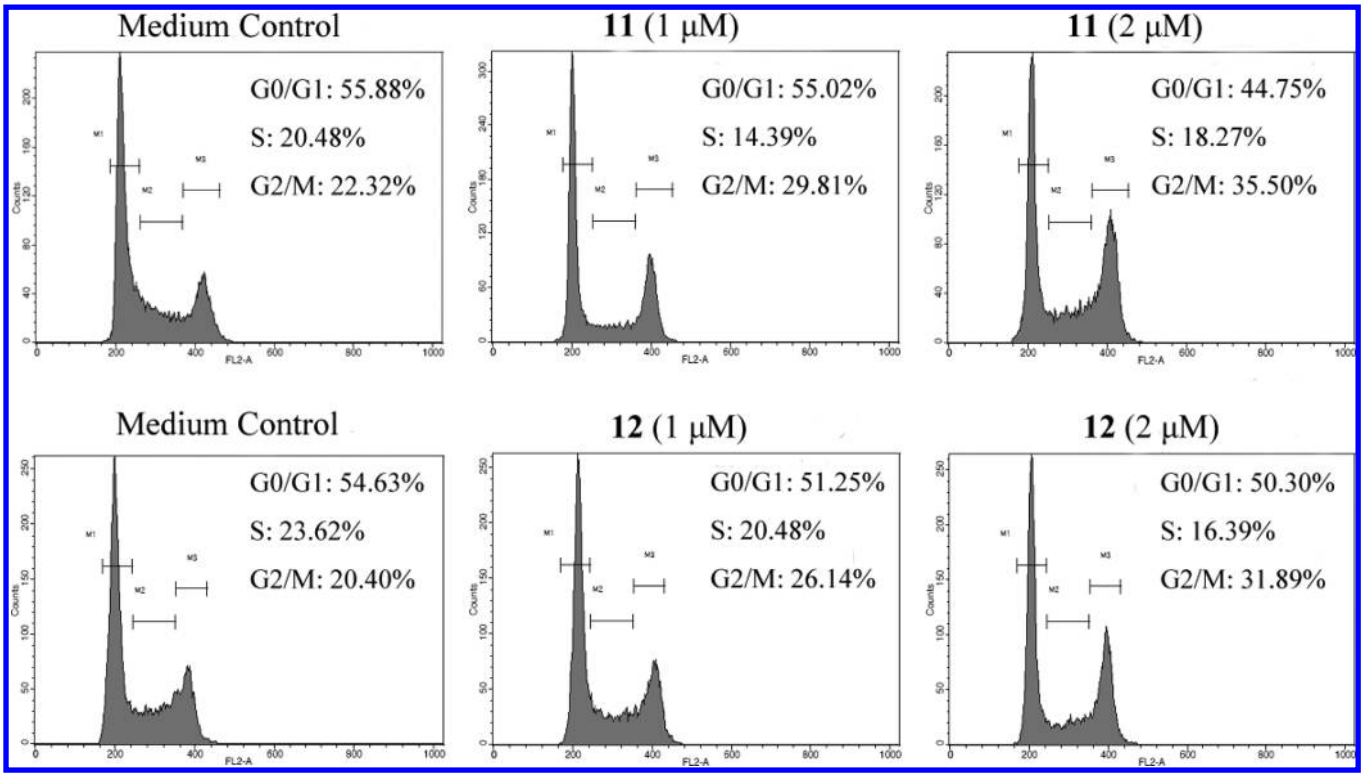

Figure 6. Compound **11** and **12** induce cell cycle arrest at G2/M phase. HCT-116 cells were treated with 1 or 2 μM compounds **11** or **12** for 12 h. Cells were fixed, stained with propidium iodide (PI), and were assessed by flow cytometry. The percentages of cells in different DNA ploidy of 2N (G0/G1), between 2N and 4N (S), and 4N (G2/M) are indicated on the right of each cell cycle profile. Data shown are from one of three independent experiments.

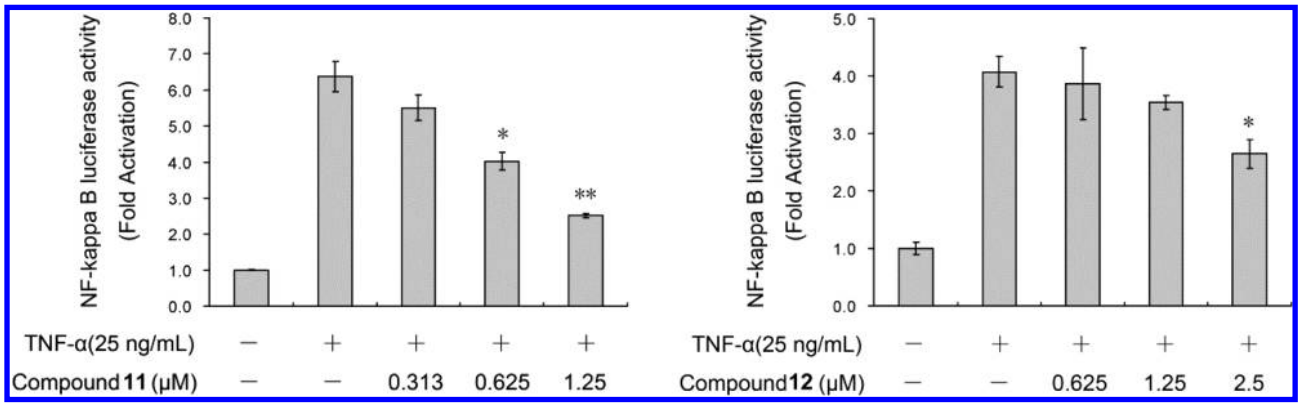

Figure 7. Inhibitory effects of compounds **11** and **12** on TNF-α-induced NF-κB activation. HEK 293T cells transiently transfected with pNFκB-luc and pRL-TK vectors were pretreated with DMSO, 0.31, 0.62, and 1.25 μM compound **11** or 0.62, 1.25, and 2.50 μM compound **12** for 1 h before TNF-α stimulation (25 ng/mL) for 18 h. The NF-κB reporter was assayed by measuring the luciferase activity as described in the Experimental Section. Data shown are from one of three independent experiments. *p < 0.05, **p < 0.01.

μM, 36.98% and 33.31%, respectively, of cell numbers were accumulated in G2/M. The percentages of cells in G0/G1 were about 55.88% and 54.63% in the untreated cells but gradually decreased to about 44.75% and 50.30% after treatment with compounds **11** and **12**, respectively. Taken together, these results indicate that **11** and **12** target tubulin directly at a different binding site from colchicine or PXL, and disrupt microtubule dynamics, which subsequently induces cell cycle arrest at prometaphase.

2.5. Inhibition of NF-κB Activation. Having validated the microtubule-interfering effects of **11** and **12**, we further evaluated their effects on the NF-κB signaling pathway. As we expected, compounds **11** and **12** suppressed TNF-α-induced NF-κB activation in a dose-dependent manner (Figure 7). Stimulation with TNF-α resulted in 6.5-fold increase in NF-κB luciferase activity over the control. TNF-α-induced NF-κB DNA binding activity was inhibited by 14%, 27%, and 37% by compound **11** at 0.31, 0.62, and 1.25 μM, respectively, and by 9%, 12%, and 28% by compound **12** at 0.62, 1.25, and 2.50 μM, respectively. We also examined the NF-κB inhibition of parthenolide (**3**) and *abeo*-docetaxel derivative **17** under the same conditions (Supporting Information Figure S3). Parthenolide (**3**) exhibited a comparable NF-κB inhibitory effect to those of **11** and **12**, while **17** showed no activity as expected. These results shown by the designed taxoids supported our initial hypothesis that an α,β-unsaturated ketone functionality is

dx.doi.org/10.1021/jm400479p | J. Med. Chem. 2013, 56, 4749−4757

an essential structural requirement for inhibition of NF-κB. To the best of our knowledge, these new taxoid derivatives are the first to exhibit TNF-α-induced NF-κB inhibitory activity.

3. CONCLUSION

In conclusion, we have demonstrated the first report of dual-functional taxoid derivatives exhibiting both microtubule destabilization and NF-κB inhibition. By incorporating essential functionalities from PXL and parthenolide into the skeleton of the inactive natural *abeo*-taxoid taxchinin A, we synthesized several new derivatives with notable selectivity against colon cancer, melanoma, and renal cancer. Mechanism of action studies revealed that these new compounds could destabilize microtubules and inhibit NF-κB activation, thereby inducing cell cycle arrest and apoptosis in tumor cells. This work provides a new strategy for future drug development based on natural taxoid scaffolds. Combination of the natural skeleton with appropriate pharmacophores has proved to be a valuable protocol for the discovery of new natural product-derived chemical entities with unique biological mechanisms. Further studies on these taxoid derivatives, including identification of the binding mode on tubulin/microtubules and the inhibitory step for suppressing NF-κB activation, are underway in our laboratories.

4. EXPERIMENTAL SECTION

4.1. Chemistry. All nonaqueous reactions were carried out under nitrogen atmosphere. Reagents were purchased from commercial sources and used as received. Dichloromethane and DMF were distilled from CaH_2, and THF was distilled from Na prior to use. ^1H and ^{13}C NMR experiments were performed on a Bruker AM-400 or DRX-500 spectrometer at ambient temperature with acetone-d_6 as the solvent. 2D NMR spectra were recorded on a Bruker DRX-500 NMR instrument. IR spectra were recorded on a Bio-Rad FTS-135 spectrometer with KBr pellets. UV spectra were obtained on a UV 2401 PC spectrometer. ESIMS and HRESIMS were taken on a VG Auto Spec-3000 or on a Finnigan MAT 90 instrument. Melting points (uncorrected) were determined on an XRC-1 micro melting point apparatus. Optical rotations were measured with a Horiba SEPA-300 polarimeter. Column chromatography was performed on silica gel (400 μ, Qingdao Marine Chemical Inc. China). The purity of all tested compounds was determined by HPLC (Agilent Technologies 1200 series) equipped with a C-18 bounded-phase column (ZORBAX, SB-C18, 4.6 mm × 250 mm). A gradient elution was performed with MeOH and water as a mobile phase and was monitored at 238 nm. All tested compounds were >95% pure.

Synthesis of Compound ***4***.[8] TBDMSCl (589 mg, 3.91 mmol) and imidazole (133.1 mg, 1.95 mmol) were added to a solution of **2** (600 mg, 0.98 mmol) in DMF (4.5 mL) at −40 °C. The reaction was stirred for 10 h at −40 °C until the starting material was consumed. The mixture was diluted with EtOAc and washed with water and brine. The organic layer was then dried (Na_2SO_4) and concentrated. The residue was purified by column chromatography (10% EtOAc in petroleum ether) to give 13-TBS-taxchinin A (672 mg, 94%).

The above product in CH_2Cl_2 (15 mL) was added to a solution of PCC (1.19 g, 5.54 mmol) in CH_2Cl_2 (15 mL). This solution was stirred for 8 h at rt. The reaction mixture was filtered and concentrated. The residue was purified by silica gel column chromatography (30% EtOAc in petroleum ether) to afford **4** (603 mg, 90%) as a white amorphous powder.

*Synthesis of 5-Oxo-taxchinin A (****5****).*[8] HF (0.75 mL, 40% aq) was added to a solution of **4** (75 mg, 0.10 mmol) in THF (14.25 mL). The reaction mixture was stirred for 2 h at room temperature (rt) and then diluted with EtOAc and treated with saturated aqueous sodium bicarbonate (10 mL). The organic layer was separated, washed with brine, dried (Na_2SO_4), and concentrated. The residue was purified by column chromatography (20% EtOAc in petroleum ether) to give **5** (55 mg, 87%) as colorless oil.

Synthesis of Compound ***6***.[8] TBAF (0.76 mL, 0.76 mmol, 1 M solution in THF) was added to a solution of **4** (500 mg, 0.69 mmol) in THF (20 mL). The reaction was stirred at rt and monitored by TLC until the starting material was consumed. The reaction mixture was diluted with EtOAc and washed with water and brine. The organic layer was dried (Na_2SO_4) and concentrated. The residue was purified by column chromatography (15% EtOAc in $CHCl_3$) to give **6** (342 mg, 90%) as yellow oil.

Synthesis of Compound ***9***. Sodium hexamethyldisilazide (NaHMDS) in THF (0.06 mL, 0.12 mmol, 2 M in THF) was added to a solution of **6** (55 mg, 0.10 mmol) and **7** (40.5 mg, 0.12 mmol) in anhydrous THF (5 mL) with stirring at −78 °C. After 30 min, the reaction was quenched with saturated aqueous NH_4Cl, and the mixture was extracted with EtOAc. The organic layer was washed with brine, dried over anhydrous Na_2SO_4, and concentrated. The residue was purified by column chromatography (25% EtOAc in petroleum ether) to give the product (96 mg) as colorless oil.

This intermediate was then dissolved in THF (35 mL) and treated with 0.5 N HCl (15 mL) at 0 °C. The reaction was allowed to warm to rt, and stirring was continued for 4 h until completion. The mixture was then diluted with EtOAc. The organic phase was washed with saturated aqueous $NaHCO_3$, brine, dried over Na_2SO_4, and concentrated. The residue was purified by column chromatography (20% EtOAc in petroleum ether) to give **9** (36 mg, 49%) as colorless oil: t_R− HPLC, 11.16 min (97.8%); $[\alpha]^{10}_D$ −29.9 (*c* 0.76, CH_3OH). UV (CH_3OH) λ_{max} (log ε) 229.8 (4.12) nm. IR (KBr) ν_{max} 3433, 2961, 2930, 2857, 1728, 1672, 1371, 1270, 1121, 1071, 1027, 713 cm^{-1}. ^1H NMR (acetone-d_6, 500 MHz) δ 7.99 (d, *J* = 10.5 Hz, 1H), 7.97 (d, *J* = 7.5 Hz, 2H), 7.92 (d, *J* = 7.5 Hz, 2H), 7.63 (t, *J* = 7.0 Hz, 1H), 7.54−7.44 (overlap, 8H), 7.31 (t, *J* = 7.0 Hz, 2H), 7.25 (t, *J* = 7.5 Hz, 1H), 6.40 (d, *J* = 11.0 Hz, 1H), 6.13−6.08 (overlap 3H), 6.08 (d, *J* = 11.0 Hz, 1H), 5.60 (dd, *J* = 9.0, 4.5 Hz, 1H), 5.56 (t, *J* = 7.5 Hz, 1H), 5.33 (s, 1H), 4.98 (d, *J* = 7.0 Hz, 1H), 4.65 (t, *J* = 4.5 Hz, 1H), 3.34 (d, *J* = 7.5 Hz 1H), 2.35−1.71 (m, 2H), 2.02 (s, 3H), 1.76 (s, 3H), 1.71 (s, 3H), 1.27 (s, 3H), 1.23 (s, 3H), 1.21 (s, 3H). ^{13}C NMR (acetone-d_6, 125 MHz) δ 189.7 s, 173.0 s, 171.8 s, 170.0 s, 167.3 s, 165.8 s, 154.8 d, 147.7 s, 143.4 s, 140.5 s, 138.4 s, 135.6 s, 134.3 d, 132.3 d, 130.6 s, 130.5 d, 129.9 d, 129.5 d, 129.2 d, 129.1 d, 128.5 d, 128.4 d, 128.3 d, 121.5 t, 80.7 d, 76.1 s, 75.4 d, 74.9 d, 70.2 d, 69.7 d, 68.7 s, 57.1 d, 48.6 d, 44.6 s, 37.9 t, 28.3 q, 27.5 q, 21.9 q, 21.7 q, 20.6 q, 12.1 q. HRMS (ESI, *m*/*z*) calcd for $C_{47}H_{49}NO_{12}Na$ $[M + Na]^+$, 842.3152; found, 842.3159.

Synthesis of Compound ***10***. Similarly to the above procedure, coupling of **8** (48.6 mg, 0.14 mmol) and **6** (40 mg, 0.07 mmol) was performed using NaHMDS (0.04 mL, 0.09 mmol, 2 M in THF), followed by removal of the C-2′ protecting groups with 0.5 N HCl (19 mL) to give **10** (26 mg, 44%) as colorless oil: t_R− HPLC, 17.92 min (98.6%); $[\alpha]^{13}_D$ −23.0 (*c* 0.31, CH_3OH). UV (CH_3OH) λ_{max} (log ε) 230.6 (3.96) nm. IR (KBr) ν_{max} 3434, 2960, 2928, 2874, 2855, 1726, 1627, 1466, 1458, 1369, 1271, 1123, 1073, 711 cm^{-1}. ^1H NMR (acetone-d_6, 500 MHz) δ 8.00 (d, *J* = 7.2 Hz, 2H), 7.65 (t, *J* = 7.2 Hz, 1H), 7.52−7.47 (overlap, 3H), 7.39−7.25 (overlap, 5H), 6.44−6.37 (overlap, 2H), 6.20−6.10 (overlap, 3H), 6.07 (s, 1H), 5.64 (t, *J* = 7.2 Hz 1H), 5.37 (s 1H), 4.49 (t, *J* = 4.8 Hz 1H), 3.38 (d, *J* = 8.1 Hz, 1H), 2.43−1.82 (m, 2H), 2.15 (s, 3H), 1.78 (s, 3H), 1.75 (3H, s), 1.39 (9H, s), 1.32 (s, 3H), 1.24 (q, 3H), 1.20 (q, 3H). ^{13}C NMR (acetone-d_6, 125 MHz) δ 189.6 s, 173.0 s, 171.9 s, 171.9 s, 170.1 s, 165.9 s, 154.9 d, 148.0 s, 143.7 s, 141.1 s, 138.4 s, 134.4 d, 130.8 s, 130.6 d, 129.9 d, 129.6 d, 129.1 d, 128.4 d, 128.2 d, 121.2 t, 80.6 d, 76.1 s, 75.5 d, 75.2 d, 70.5 d, 69.9 d, 68.9 s, 58.1 d, 55.6 s, 48.8 d, 44.8 s, 37.9 t, 28.7 q, 28.5 q, 27.6 q, 22.1 q, 22.1 q, 20.6 q, 12.2 q. HRMS (ESI, *m*/*z*) calcd for $C_{45}H_{53}NO_{13}Na$ $[M + Na]^+$, 838.3414; found, 838.3412.

Conversion of Compound ***5*** *into Compounds* ***11*** *and* ***9***. Using the same procedure as for **9**, compounds **7** (41.9 mg, 0.12 mmol) and **5** (63 mg, 0.10 mmol) were coupled with the use of NaHMDS (0.06 mL, 0.12 mmol, 2 M in THF), followed by removal of the protecting groups at C-2′ with 0.5 N HCl (19 mL) to give **11** (20 mg, 22%) and **9** (23 mg, 27%).

dx.doi.org/10.1021/jm400479p | J. Med. Chem. 2013, 56, 4749−4757

Compound ***11***. Colorless oil. t_R− HPLC, 11.30 min (97.3%); $[\alpha]^{10}_D$ 37.5 (*c* 0.39, CH_3OH). UV (CH_3OH) λ_{max} (log ε) 227.6 (4.14) nm. IR (KBr) ν_{max} 3434, 2955, 2871, 1726, 1670, 1640, 1466, 1385, 1368, 1272, 1241, 1042, 990, 711 cm^{-1}. ^1H NMR (acetone-d_6, 500 MHz) δ 8.02−8.00 (overlap, 3H), 7.97 (d, *J* = 7.5 Hz, 2H), 7.62 (t, *J* = 7 Hz, 1H), 7.56−7.48 (overlap, 7H), 7.38 (t, *J* = 8.0 Hz, 2H), 7.29 (t, *J* = 7.5 Hz, 1H), 6.12 (br s, 1H), 5.85 (s, 1H), 5.80 (s, 1H), 5.77 (t, *J* = 7.5 Hz, 1H), 5.55 (s, 1H), 5.15 (br s, 1H), 5.24 (br s, 1H), 4.82 (s, 1H), 3.37 (d, *J* = 7.5 Hz, 1H), 2.61−2.54 (overlap, 2H), 2.34 (m, 1H), 2.05 (s, 3H), 1.29 (s, 3H), 1.14 (s, 3H), 1.96 (s, 3H), 1.92 (s, 3H), 2.34−1.74 (m, 4H), 0.96 (s, 3H). ^{13}C NMR (acetone-d_6, 125 MHz) δ 198.3 s, 173.2 s, 170.5 s, 170.4 s, 170.4 s, 167.4 s, 166.3 s, 147.7 s, 141.0 s, 141.0 s, 144.9 s, 135.7 s, 133.9 d, 132.4 d, 131.4 s, 130.6 d, 129.4 d, 129.3 d, 129.2 d, 128.8 t, 128.4 d, 128.2 d, 128.2 d, 82.2 d, 75.8 s, 75.4 d, 74.8 d, 71.0 d, 70.6 d, 70.1 d, 69.8 s, 56.5 d, 43.9 s, 42.9 d, 38.3 t, 39.4 t, 28.9 q, 28.2 q, 22.1 q, 21.0 q, 21.0 q, 13.1 q, 12.1 q. HRMS (ESI, *m*/*z*) calcd for $C_{49}H_{53}NO_{14}Na$, 902.3363 $[M + Na]^+$; found, 902.3359.

Conversion of Compound ***5*** *into Compounds* ***12*** *and* ***10***. Coupling of compounds **8** (32.8 mg, 0.10 mmol) and **5** (50 mg, 0.08 mmol) using NaHMDS (0.05 mL, 0.10 mmol, 2 M in THF) was performed with the same procedure as for **9**. Subsequent removal of the protecting groups at C-2′ with 0.5 N HCl (15 mL) gave **12** (18 mg, 25%) and **10** (23 mg, 34%).

Compound ***12***. Colorless oil. t_R− HPLC, 19.31 min (98.1%); $[\alpha]^{18}_D$ 16.3 (*c* 0.24, CH_3OH). UV (CH_3OH) λ_{max} (log ε) 228.4 (3.60) nm. IR (KBr) ν_{max} 3433, 2960, 2925, 2874,2853, 1729, 1629, 1466, 1369, 1273, 1247, 1124, 1073, 745, 707 cm^{-1}. ^1H NMR (acetone-d_6, 500 MHz) δ 8.03 (d, *J* = 8.0 Hz, 2H), 7.62 (t, *J* = 7.5 Hz, 1H), 7.50 (t, *J* = 7.5 Hz, 2H), 7.45 (d, *J* = 7.5 Hz, 2H), 7.36 (t, *J* = 7.5 Hz, 2H), 7.28 (t, *J* = 7.0 Hz, 1H), 6.40 (d, *J* = 10.0 Hz, 1H), 6.15 (br s, 1H), 5.92 (d, *J* = 7.5 Hz, 1H), 5.87−5.85 (overlap, 2H), 5.59 (s, 1H), 5.31 (d, *J* = 10.0 Hz, 1H), 5.24 (m, 1H), 4.53 (br s, 1H), 3.44 (d, *J* = 7.5 Hz, 1H), 2.57−1.92 (m, 4H), 2.05 (s, 3H), 1.96 (s, 3H), 1.93 (s, 3H), 1.90 (s, 3H), 1.45 (s, 9H), 1.29 (s, 3H), 1.19 (s, 3H), 1.00 (s, 3H). ^{13}C NMR (acetone-d_6, 125 MHz) δ 198.3 s, 173.1 s, 170.7 s, 170.5 s, 170.3 s, 167.7 s, 165.8 s, 147.9 s, 145.2 s, 142.5 s, 136.3 s, 133.9 d, 131.5 s, 130.7 d, 129.4 d, 129.2 d, 128.2 d, 128.0 d, 126.5 t, 82.2 d, 75.8 s, 75.0 d, 74.9 d, 71.1 d, 70.8 d, 70.2 d, 66.9 s, 57.5 d, 55.4 s, 44.0 s, 43.0 d, 39.5 t, 38.2 t, 29.1 q, 28.8 q, 28.3 q, 22.3 q, 21.1 q, 21.0 q, 13.2 q, 12.0 q. HRMS (ESI, *m*/*z*) calcd for $C_{47}H_{57}NO_{15}Na$ $[M + Na]^+$, 898.3625; found, 898.3624.

Synthesis of Compound ***13***. Using the same procedure as for **9**, coupling of compounds **7** (66 mg, 0.20 mmol) and **2** (100 mg, 0.16 mmol) was performed with NaHMDS (0.10 mL, 0.20 mmol). Removal of the C-2′ protecting groups with 0.5 N HCl (37 mL) gave **13** (73 mg, 51%) as colorless oil. t_R− HPLC, 17.37 min (96.9%); $[\alpha]^{18}_D$ −22.9 (*c* 0.37, CH_3OH). UV (CH_3OH) λ_{max} (log ε) 228.4 (3.80) nm. IR (KBr) ν_{max} 3430, 2958, 2926, 2872, 2855, 1732, 1465, 1374, 1376, 1270, 1252, 1221, 1173, 1122, 1072, 1029, 746, 711 cm^{-1}. ^1H NMR (acetone-d_6, 500 MHz) δ 7.91 (d, *J* = 7.5 Hz, 2H), 7.64 (t, *J* = 7.2 Hz,1H), 7.51 (t, *J* = 7.5 Hz, 2H), 7.45 (d, *J* = 7.5 Hz, 2H), 7.34 (t, *J* = 7.0 Hz, 2H), 7.25 (t, *J* = 7.5 Hz, 1H), 6.63 (d, *J* = 10.5 Hz,1H), 6.55 (br s, 1H), 6.19 (d, *J* = 8.0 Hz 1H), 6.07 (d, *J* = 10.5 Hz,1H), 5.55 (m, 1H), 5.34 (s, 1H), 4.96 (s, 1H), 4.72−4.69 (overlap, 3H), 3.41 (d, *J* = 8.0 Hz, 1H), 2.60−2.46 (m, 2H), 2.16 (s, 3H), 2.14−2.08 (m, 2H), 2.05 (s, 3H), 2.02 (s, 3H), 1.78 (s, 3H), 1.40 (s, 9H), 1.29 (s, 3H), 1.19 (s, 3H), 1.07 (s, 3H). ^{13}C NMR (acetone-d_6, 125 MHz) δ172.1 s, 171.8 s, 170.4 s, 170.4 s, 170.0 s, 165.0 s, 153.8 s, 141.5 s, 141.5 s, 134.3 d, 134.1 s, 130.3 s, 130.3 d, 129.7 d, 129.1 d, 128.1 d, 128.0 d, 115.7 t, 77.7 d, 77.2 d, 77.0 d, 75.8 s, 75.6 d, 70.9, d, 69.6 d, 69.3 s, 68.4 d, 58.0 d, 55.6 s, 46.0 s, 44.0 d, 41.1 t, 35.6 t, 28.7 q, 28.3 q, 27.1 q, 22.1 q, 21.5 q, 20.9 q 14.0 q, 12.5 q. HRMS (ESI, *m*/*z*) calcd for $C_{47}H_{59}NO_{15}Na$ $[M + Na]^+$, 900.3782; found, 900.3787.

Oxidation of Compound ***13*** *to* ***14***. PCC (78 mg, 0.36 mmol) in CH_2Cl_2 (8 mL) was added to a solution of **13** (53 mg, 0.06 mmol) in CH_2Cl_2 (10 mL). The reaction was stirred at rt and monitored by TLC until the starting material was consumed. The mixture was filtered and concentrated. The residue was purified by silica gel column chromatography (40% EtOAc in petroleum ether) to afford **14** (28 g, 53%) as colorless oil: t_R− HPLC, 24.32 min (98.6%); $[\alpha]^{18}_D$ 37.0 (*c* 0.55, CH_3OH). UV (MeOH) λ_{max} (log ε) 235.0 (3.97) nm. IR (KBr) ν_{max} 3443, 2962, 2929, 2874, 2857, 1724, 1602, 1497, 1468, 1454, 1370, 1272, 1239, 1174, 1120, 1071, 1027, 981, 917, 747, 706 cm^{-1}. ^1H NMR (acetone-d_6, 500 MHz) δ 8.01 (d, *J* = 7.0 Hz, 2H), 7.62 (t, *J* = 7.0 Hz, 1H), 7.50 (t, *J* = 7.5 Hz, 2H), 7.45 (d, *J* = 7.5 Hz, 2H), 7.34 (t, *J* = 6.5 Hz, 2H), 7.25 (t, *J* = 7.0 Hz, 1H), 6.37 (d, *J* = 9.0 Hz,1H), 6.26−6.12 (overlap, 2H), 5.70 (br s, 1H), 5.50 (s, 1H), 5.12 (br s, 1H), 5.03 (s, 1H), 4.96 (br s, 1H), 4.60 (br s, 1H), 3.06 (d, *J* = 9.0 Hz, 1H), 2.73−1.70 (m, 4H), 2.06 (s, 3H), 1.98 (s, 3H), 1.93 (s, 3H), 1.91 (s, 3H), 1.37 (s, 9H), 1.28 (s, 3H), 1.19 (s, 3H), 1.17 (s, 3H). ^{13}C NMR (acetone-d_6, 125 MHz) δ 206.8 s, 174.4 s, 171.7 s, 170.8 s, 170.4 s, 170.4 s, 166.7 s, 162.1 s, 148.4 s, 141.4 s, 133.9 d, 131.4 s, 130.6 d, 129.4 d, 129.1 d, 128.1 d, 128.0 d, 116.1 t, 76.1 s, 75.3 d, 74.9 d, 71.8 d, 70.8 d, 70.1, d, 69.2 d, 63.3 s, 57.5 d, 55.6 s, 46.4 d, 45.1 s, 44.6 t, 33.5 t, 29.1 q, 28.6 q, 27.3 q, 21.7 q, 21.0 q, 20.9 q, 15.2 q, 9.5 q. HRMS (ESI, *m*/*z*) calcd for $C_{47}H_{57}NO_{15}Na$ $[M + Na]^+$, 898.3625; found, 898.3628.

Synthesis of Compounds ***16*** *and* ***17***. Compounds **16** and **17** were prepared from **15** following the procedures described in our previous paper.[14]

4.2. NCI-60 Human Tumor Cell Line Screening. Compounds were evaluated in the NCI's human tumor 60-cell line screening, and data calculations were performed as described.[15]

4.3. Apoptosis Assay. HCT-116 cells were treated with increasing amounts of compound **11** or **12** for 24 h, washed with phosphate buffered saline (PBS), and after trypsinization, apoptosis was evaluated using annexin V-fluorescein 5-isothiocyanate (annexin V-FITC)/propidium iodine (PI) staining with an Annexin V-FITC apoptosis detection kit (BD Biosciences, San Jose, USA). Samples were analyzed by flow cytometry using FACSCalibur and CellQuest software (Becton Dickinson). Co-staining with Annexin V and PI allows classification of viable cells (Annexin V-negative, PI-negative) from early apoptotic cells (Annexin V-positive, PI-negative) and late apoptotic or necrotic cells (Annexin V-positive, PI-positive).

4.4. Tubulin Polymerization Assay. The effects of compounds on tubulin polymerization were determined by tubulin polymerization assay kit (Cytoskeleton, Denver, CO, USA). Standards and tested compounds were mixed with tubulin according to manufacturer's instructions. Fluorescence was detected by a temperature regulated fluorimeter capable of reading at 410−460 nm in kinetic mode using excitation filters of 340−360 nm. The resulting polymerization curve is representative of the three phases of microtubules polymerization, namely nucleation, growth, and steady state equilibrium. Compounds or proteins that interact with tubulin will often alter one or more of the characteristic phases of polymerization.

4.5. Immunofluorescence Staining of Tubulin. PC-3 cells were grown on 8-well chamber slide (Lab-Tech) for 36 h prior to treatment with DMSO (control), 2 or 10 μM compound **11**, 5 or 10 μM compound **12**, 200 nM CA4, or 200 nM PXL for 24 h. Cells were fixed in 4% paraformaldehyde in PBS, and permeabilized with 0.5% Triton X-100 in PBS. Cells were labeled with mouse monoclonal antibody to α-tubulin (B5−1−2, Sigma), followed by FITC conjugated secondary antibody (Sigma).[17] Nuclei were labeled with DAPI. Fluorescence labeled cells were observed using an Olympus BX61 fluorescence microscope, and images were captured by an ORCA-R^2 digital camera (Hamamatsu Photonics) controlled by Volocity 5.5.2 software (Perkin-Elmer Inc.) (Microscopy Service Laboratory, UNC−CH). Final images were prepared using Adobe Photoshop.

4.6. Cell Cycle Analysis. Cell cycle was evaluated by measurement of the DNA content by PI (St Louis, MO) staining. Briefly, HCT-116 cells were seeded in six-well plates at a density of 5×10^5 cells/well 24 h prior to treatment with compounds **11** or **12**. After 12 h, cells and supernatants were collected together, centrifuged at 1000 rpm for 5 min, and pelleted. The pellet was resuspended and fixed with 70% EtOH overnight at 4 °C. After being stained with PI, cells were subjected to flow cytometric cell cycle analysis. Experiments were repeated a minimum of two times.

4.7. Luciferase Reporter Assay. HEK 293T cells were transiently transfected with pNFκB-luc (Beyotime) and pRL-TK (Promega,

Madison, WI) vectors using Lipofectamine 2000 transfection reagent (Invitrogen) for 12 h. The cells were then preincubated with different concentrations of compound for 1 h and were subsequently activated with TNF-α for 18 h. Transcriptional activity was determined by measuring the activities of firefly and *Renilla reniformis* luciferases in Luminoskan Ascent microplate luminometer (Thermo Scientific) using Dual-Luciferase Reporter Assay (Promega) according to the manufacturer's instructions.

■ ASSOCIATED CONTENT

Ⓢ Supporting Information

Growth inhibitory activity of compounds **9**−**12** against a panel of 60 human tumor cell lines, effects of compounds **11**, **12**, PXL, and CA4 on microtubule dynamics in PC-3 cells, and inhibitory effects of compounds **3** and **17** on TNF-α-induced NF-κB activation. This material is available free of charge via the Internet at http://pubs.acs.org.

■ AUTHOR INFORMATION

Corresponding Author

*For Q.-S.Z.: phone, 86 871-5223058; fax, 86 871-5215783; E-mail, qinshizhao@mail.kib.ac.cn. For Z.-J.Y.: phone, 86 21-54925133; fax, 86 21-64166128; E-mail, yaoz@mail.sioc.ac.cn. For K.-H.L.: phone, 919-962-0066; fax, 919-966-3893; E-mail, khlee@unc.edu.

Author Contributions

▽These authors contributed equally to this paper

Notes

The authors declare no competing financial interest.

■ ACKNOWLEDGMENTS

We thank the U.S. National Cancer Institute for screening of 60 human tumor cell lines (NCI-60). This work was supported by the National Natural Science Foundation of China (81172941, 21032002, 20802083, and 90813004) and the Ministry of Science and Technology (2011CB915503 and 2009CB522303). Support was also due in part to NIH grant CA177584 from the National Cancer Institute awarded to K. H. Lee.

■ ABBREVIATIONS USED

CA4, combretastatin A4; CNS, central nervous system; DAPI, 4′,6-diamidino-2-phenylindole; FITC, fluorescein 5-isothiocyanate (FITC); GI_{50}, (50% growth inhibition); NaHMDS, sodium hexamethyldisilazide; National Cancer Institute; PBS, phosphate buffered saline; PCC, pyridinium chlorochromate; PI, propidium iodine; PXL, paclitaxel; SAR, structure−activity relationship; TBAF, tetra-*n*-butylammonium fluoride; TBDMSCl, *tert*-butyldimethylchlorosilane

■ REFERENCES

(1) (a) Newman, D. J. Natural products as leads to potential drugs: an old process or the new hope for drug discovery? *J. Med. Chem.* **2008**, *51*, 2589−2599. (b) Mann, J. Natural products in cancer chemotherapy: past, present and future. *Nature Rev. Cancer* **2002**, *2*, 143−148.

(2) Petrelli, A.; Giordano, S. From single- to multi-target drugs in cancer therapy: when aspecificity becomes an advantage. *Curr. Med. Chem.* **2008**, *15*, 422−432.

(3) Morphy, R.; Rankovic, Z. Designing multiple ligands—medicinal chemistry strategies and challenges. *Curr. Pharm. Des.* **2009**, *15*, 587−600.

(4) Schiff, P. B.; Fant, J.; Horwitz, S. B. Promotion of microtubule assembly invitro by taxol. *Nature* **1979**, *277*, 665−667.

(5) Kingston, D. G. I. Taxol, a molecule for all seasons. *Chem. Commun.* **2001**, 867−880.

(6) (a) Baloglu, E.; Kingston, D. G. I. The taxane diterpenoids. *J. Nat. Prod.* **1999**, *62*, 1448−1472. (b) Shigemori, H.; Kobayashi, J. Biological activity and chemistry of taxoids from the Japanese yew *Taxus cuspidata*. *J. Nat. Prod.* **2004**, *67*, 245−256. (c) Li, S. H., Taxoids. In *The Chemistry of Diterpenoids*, 1st ed.; Sun, H. D., Li, S. H., Eds; Chemical Industry Press: Beijing, 2011; pp 278−366.

(7) (a) Samaranayake, G.; Magri, N. F.; Jitrangsri, C.; Kingston, D. G. I. Modified taxols. 5. Reaction of taxol with electrophilic reagents and preparation of a rearranged taxol derivative with tubulin assembly activity. *J. Org. Chem.* **1991**, *56*, 5114−5119. (b) Qin, Y.; Fang, Q. C.; Liang, X. T. Semisynthesis and biological evaluation of taxayuntin 13-[*N*-benzoyl-(2′*R*,3′*S*)-3′-phenylisoserinate]. *Chin. Chem. Lett.* **1996**, *7*, 886−887. (c) Chordia, M. D.; Kingston, D. G. I.; Hamel, E.; Lin, C. M.; Long, B. H.; Fairchild, C. A.; Johnston, K. A.; Rose, W. C. Synthesis and biological activity of A-nor-paclitaxel analogues. *Bioorg. Med. Chem.* **1997**, *5*, 941−947. (d) Tremblay, S.; Soucy, C.; Towers, N.; Gunning, P. J.; Breau, L. Characterization of an *abeo*-taxane: brevifoliol and derivatives. *J. Nat. Prod.* **2004**, *67*, 838−845. (e) Tang, S. B.; Yang, C.; Brodie, P.; Bane, S.; Ravindra, R.; Sharma, S.; Jiang, Y.; Snyder, J. P.; Kingston, D. G. I. Bridging converts a noncytotoxic nor-paclitaxel derivative to a cytotoxic analogue by constraining it to the T-taxol conformation. *Org. Lett.* **2006**, *8*, 3983−3986.

(8) Zhao, Y.; Guo, N.; Lou, L. G.; Cong, Y. W.; Peng, L. Y.; Zhao, Q. S. Synthesis, cytotoxic activity, and SAR analysis of the derivatives of taxchinin A and brevifoliol. *Bioorg. Med. Chem.* **2008**, *16*, 4860−4871.

(9) Karin, M. Nuclear factor-[kappa]B in cancer development and progression. *Nature* **2006**, *441*, 431−436.

(10) (a) Bentires-Alj, M.; Barbu, V.; Fillet, M.; Chariot, A.; Relic, B.; Jacobs, N.; Gielen, J.; Merville, M. P.; Bours, V. NF-kappaB transcription factor induces drug resistance through MDR1 expression in cancer cells. *Oncogene* **2003**, *22*, 90−97. (b) Baldwin, A. S. Control of oncogenesis and cancer therapy resistance by the transcription factor NF-kappa B. *J. Clin. Invest.* **2001**, *107*, 241−246.

(11) Shen, H. M.; Tergaonkar, V. NF kappa B signaling in carcinogenesis and as a potential molecular target for cancer therapy. *Apoptosis* **2009**, *14*, 348−363.

(12) (a) Gao, Z. W.; Zhang, D. L.; Guo, C. B. Paclitaxel efficacy is increased by parthenolide via nuclear factor-kappaB pathways in in vitro and in vivo human non-small cell lung cancer models. *Curr. Cancer Drug Targets* **2010**, *10*, 705−715. (b) Sohma, I.; Fujiwara, Y.; Sugita, Y.; Yoshioka, A.; Shirakawa, M.; Moon, J. H.; Takiguchi, S.; Miyata, H.; Yamasaki, M.; Mori, M.; Doki, Y. Parthenolide, an NF-kappaB inhibitor, suppresses tumor growth and enhances response to chemotherapy in gastric cancer. *Cancer Genomics Proteomics* **2011**, *8*, 39−47. (c) Ganta, S.; Amiji, M. Coadministration of paclitaxel and curcumin in nanoemulsion formulations to overcome multidrug resistance in tumor cells. *Mol. Pharmaceutics* **2009**, *6*, 928−939.

(13) Ghantous, A.; Gali-Muhtasib, H.; Vuorela, H.; Saliba, N. A.; Darwiche, N. What made sesquiterpene lactones reach cancer clinical trials? *Drug Discovery Today* **2010**, *15*, 668−678.

(14) Zhao, Y.; Zhang, H. B.; Liu, J. K.; Su, J.; Li, Y.; Yao, Z. J.; Zhao, Q. S. Fragmentations of 13-oxo-taxyunnansin A and their application to preparation of *abeo*-paclitaxel and *abeo*-docetaxel analogues. *Tetrahedron Lett.* **2011**, *52*, 139−142.

(15) Shoemaker, R. H. The NCI60 human tumour cell line anticancer drug screen. *Nature Rev. Cancer* **2006**, *6*, 813−823.

(16) Altmann, K. H.; Gertsch, J. Anticancer drugs from nature—natural products as a unique source of new microtubule-stabilizing agents. *Nat. Prod. Rep.* **2007**, *24*, 327−357.

(17) Nakagawa-Goto, K.; Wu, P. C.; Lai, C. Y.; Hamel, E.; Zhu, H.; Zhang, L.; Kozaka, T.; Ohkoshi, E.; Goto, M.; Bastow, K. F.; Lee, K. H. Antitumor agents. 284. New desmosdumotin B analogues with bicyclic B-ring as cytotoxic and antitubulin agents. *J. Med. Chem.* **2011**, *54*, 1244−1255.